

IDA

INSTITUTE FOR DEFENSE ANALYSES

**Antitank and Antipersonnel Mine Detection
Test Results for a Nuclear Quadrupole
Resonance Detection System**

Frank S. Rotondo
Elizabeth Ayers

March 2000

Approved for public release;
distribution unlimited.

IDA Document D-2444

Log: H 00-000567

20000615 031

DTIC QUALITY INSPECTED 4

This work was conducted under contract DASW01 98 C 0067, Task DA-2-1698, for the Defense Advanced Research Projects Agency. The publication of this IDA document does not indicate endorsement by the Department of Defense, nor should the contents be construed as reflecting the official position of that Agency.

© 2000 Institute for Defense Analyses, 1801 N. Beauregard Street, Alexandria, Virginia 22311-1772 • (703) 845-2000.

This material may be reproduced by or for the U.S. Government pursuant to the copyright license under the clause at DFARS 252.227-7013 (NOV 95).

INSTITUTE FOR DEFENSE ANALYSES

IDA Document D-2444

**Antitank and Antipersonnel Mine Detection
Test Results for a Nuclear Quadrupole
Resonance Detection System**

Frank S. Rotondo
Elizabeth Ayers

PREFACE

This document summarizes the results of an interim test of a system that uses the nuclear quadrupole resonance signature of explosives for the detection of antipersonnel and antitank landmines. The system, designed and built by Quantum Magnetics, Inc., of San Diego, California, has been funded by the Defense Advanced Research Projects Agency (DARPA) "Dog's Nose Program" to develop technologies using chemical-specific approaches to the detection of explosives. The tests, performed the weeks of October 25 and November 29, 1999, took place at the DARPA Test Site at Fort Leonard Wood, near St. Robert, Missouri.

This document was prepared for DARPA under a task entitled "Mine and UXO Detection."

CONTENTS

EXECUTIVE SUMMARY	ES-1
I. INTRODUCTION.....	I-1
A. Test Background.....	I-1
B. The NQR Approach to Mine Detection	I-2
C. Hardware Configuration Used at the Test.....	I-6
D. Measures of Effectiveness.....	I-8
II. ANTITANK MINE TEST RESULTS	II-1
A. Test Procedures	II-1
B. Analysis Overview	II-3
C. False-Alarm Rate Projection	II-5
D. Detection Probability.....	II-6
E. Alternate TNT Threshold on the West Lane	II-8
F. Range of Scans	II-8
G. Issues Affecting Vehicle Speed.....	II-9
III. SHALLOW ANTIPERSONNEL MINE TEST RESULTS.....	III-1
A. Test Structure	III-1
B. Analysis Overview	III-2
C. TNT <i>FAR</i> and P_d	III-3
D. RDX <i>FAR</i> and P_d	III-5
E. Survey Speed.....	III-6
IV. DEEP ANTIPERSONNEL MINE TEST RESULTS	IV-1
A. Test Procedure.....	IV-1
B. <i>FAR</i>	IV-1
C. Detection Probability.....	IV-1
D. Survey Speed.....	IV-2

V. RESULTS SUMMARY AND CONCLUSIONS	V-1
A. Vehicular AT Performance Projections	V-1
B. Hand-held Performance on Shallow AP Mines	V-1
C. Hand-held Performance on Deep AP Mines	V-2
D. Final Remarks	V-2

FIGURES

I-1.	(a) A Schematic View of a Quadrupole Nucleus (b) The Low-Energy and High-Energy Configurations of a Quadrupole in an Electric Field Gradient	I-2
I-2.	The Interaction of a Nuclear Quadrupole with an Axially Symmetric Field Gradient.....	I-3
I-3.	(a) The Torque of an Alternating Magnetic Field at the NQR Frequency on the Magnetic Moments Precessing About the z -Axis in the Explosive Sample (b) The Moments Rotating in the x - y plane is the Result of a $\pi/2$ Rotation of the Moments.....	I-4
I-4.	The Quantum Magnetics NQR Test at Fort Leonard Wood	I-7
II-1.	Quantum Magnetics Did Not Survey the AT Lane in a Sequential Manner.....	II-2
II-2.	The On-Axis Magnetic Field Strength (normalized) and Inhomogeneity ($dB/dZ/B$) for a Simple Wire Coil of Radius R	II-4
II-3.	Illustration of the 90-percent Fill-Factor Requirement to Determine per-Footprint Detection Probability	II-7
II-4.	TNT Signal Recorded for N_{full} Cells vs. N_{MT} Cells	II-9
II-5.	(A) TNT, (B) RDX, and (C) Metal Signal Measured vs. Miss Distance to the Nearest Mine	II-10
III-1.	Results of Single Passes (a) and Scan/Confirm Scheme (b) on Seven PMA-1A TNT-Filled AP Mines	III-4
III-2.	Results of Single Passes on Five VS-50 RDX-Filled AP Mines	III-5
III-3.	Histogram of RDX Data for Footprints Not Near a VS-50	III-7
III-4.	Results of Single Passes (a) and Scan/Confirm Scheme (b) on Five VS-50 RDX-filled AP Mines	III-7

TABLES

I-1.	NQR Parameters for TNT and RDX	I-6
II-1.	Summary of the AT Mines Used in the Test.....	II-1
II-2.	Summary of the P_{fa} Measured in This Test as well as the Projected FAR for a Vehicular System Whose Cell Area, A_{proj} , Is yet to Be Determined.....	II-6
II-3.	Summary of P_d Results on the East and West Lanes.....	II-8
III-1.	A Summary of the AP Mines Used in the Test	III-1
III-2.	Summary of the TNT Results.....	III-4
III-3.	Summary of the RDX Results	III-8
V-1.	A Summary of the AT Performance Estimates for a Vehicular System	V-1
V-2.	A Summary of the Hand-held System's Shallow AP Performance	V-1
V-3.	A Summary of the Hand-held System's Deep AP Performance.....	V-2

EXECUTIVE SUMMARY

BACKGROUND

This report summarizes the results of an interim test of a system that uses the nuclear quadrupole resonance (NQR) signature of explosives for the detection of antipersonnel (AP) and antitank (AT) landmines. The system, designed and built by Quantum Magnetics, Inc. of San Diego, California, has been funded by the Defense Advanced Research Projects Agency (DARPA) Dog's Nose Program to develop technologies using chemical-specific approaches for the detection of explosives.

The tests discussed herein, performed the weeks of October 25 and November 29, 1999, took place at the DARPA Test Site at Ft. Leonard Wood near St. Robert, Missouri. The Quantum Magnetics system was tested against AP and AT mines buried in a set of test lanes. The AT mines were either plastic or metal cased and filled with either TNT or Comp B (which is a roughly equal mixture of TNT and RDX); the AP mines were plastic cased and filled with either TNT or RDX. Although the system tested here was a hand-held device, the goal of the test was to understand the current state of effectiveness that the NQR system would have as both a vehicle-mounted and hand-held system. Specifically, the test addressed three capabilities: (1) how a vehicle-mounted system would perform on AT targets, (2) how a hand-held system would perform on shallow AP targets, and (3) how a hand-held system would perform on deep AP targets.

The Quantum Magnetics system is currently configured to detect TNT and RDX, the two most common explosives used in landmines. The NQR frequencies used for these substances are about 842 kHz and 3.41 MHz, respectively. Since no other known substances have the same NQR resonance frequencies, there are no known clutter sources that could cause false alarms in the system. The system is limited, however, by radio frequency interference (RFI) sources that can reduce sensitivity and cause false alarms. This is especially true of TNT, whose resonance near 842 kHz is located in the AM radio band.

The system used at the tests consisted of a hand-held search head tethered to an electronics trailer that was towed by an automobile. The diameter of the search head's circular coil was 40 cm, although its effective footprint (or "sweet spot") was a circle of

diameter 14 cm. The same search head was used to transmit (excite the NQR modes) and receive the NQR signal from the ground beneath the detector. The electronics trailer, which was powered by a portable diesel generator, contained signal-processing and data-acquisition hardware. An RFI mitigation system was also implemented during the test. It consisted of RFI mitigation software and a multi-axis antenna to detect ambient RF energy.

ANTITANK MINE DETECTION

The first test was designed to provide results necessary to predict the performance of a future vehicle-mounted NQR system against AT mines. The test lane was sectioned into an 8 by 192 cell array, where the cell length and width was set equal to the device's effective footprint diameter of 14 cm, hence the total lane area was about 30 m². The lane contained 1 TMM-1, 2 Type 72, and 20 TMA-4 mines. Each mine was buried under dirt such that the top of the mine was between 2.5 and 5 cm below ground surface. The mines were randomly distributed in the lane (they were not positioned relative to the established cell locations). Table ES-1 contains details on these mines.

Table ES-1. A Summary of the AT Mines Used in the Test.
The quantities *d* and *h* stand for diameter and height.

AT Model	Case Material	Main Charge	Size (cm)	Country of Origin
TMA-4	plastic	5.5 kg TNT	<i>d</i> = 28.4, <i>h</i> = 11	former Yugoslavia
Type 72	plastic	5.4 kg TNT/RDX (50.50)	<i>d</i> = 27, <i>h</i> = 10	China
TMM-1	metal	5.6 kg TNT	<i>d</i> = 30, <i>h</i> = 9	former Yugoslavia

Assumptions must be made to extrapolate from the system tested here and a future vehicular system. Because the size of the coils for a vehicular system has not yet been determined, we leave their single-coil area as a variable in the predicted results for a vehicle system. We do assume, however, that the coils will achieve the same signal-to-clutter separation as the coil tested herein and that the coils' diameter will be of order or larger than a mine's. Table ES-2 summarizes the antitank system false-alarm rate (*FAR*) and detection probability (*P_d*) performance estimates using a single 0.25 s TNT scan, a single 1 s RDX scan, and a single metal scan; the variable *A_{proj}* is the projected cell area that is surveyed by a single placement of the future vehicle coil. The two estimates presented for TNT correspond to two different TNT thresholds considered by the

contractor during the test. An estimate of the survey speed is not possible from this test because the vehicle design has not yet been determined.

Table ES-2. A Summary of the AT Performance Estimates for a Vehicular System

Antitank Test Summary

Scan Type	$FAR (m^{-2})$	P_d
TNT (thresholds set at test)	$0.021/A_{proj}$	0.81
TNT (east threshold applied)	$0.039/A_{proj}$	0.89
RDX (thresholds set at test)	$0.0054/A_{proj}$	1
Metal (thresholds set at test)	$0.0009/A_{proj}$	1

SHALLOW ANTIPERSONNEL MINE DETECTION

The second test evaluated hand-held system performance against shallow AP mines. The test lane was arranged to be 8 cells wide by 32 cells long. Again, the size of the cell edge was set equal to the effective footprint diameter (14 cm), so the total lane area was 5.02 m². The lane contained five VS-50 and seven PMA-1A mines; each mine in this lane was buried such that the top of the mine was roughly flush with the ground surface. Table ES-3 contains details on these mines.

Table E-3. A Summary of the AP Mines Used in the Test. The quantities d, h, l, and w stand for diameter, height, length, and width.

AP Model	Case Material	Main Charge	Size (cm)	Country of Origin
PMA-1A	plastic	200 g TNT	$l = 14, w = 7, h = 3$	former Yugoslavia
VS-50	plastic	43 g RDX	$d = 9, h = 4.5$	Italy

Because the search head used in the test was akin to a hand-held device, the performance projection to a future hand-held system is straightforward. The results in this report are based on a complete scan of the test lane followed by a confirmation scan of only those positions that exceeded a preset threshold on the first scan of the lane. In this approach, a mine declaration would be made when both scans exceeded the threshold. This scan/confirm approach was necessary because the signal-to-noise on AP mines, especially those that are TNT-filled, is small (recall that only single scans were used to obtain the AT results above because the signals available from AT mines were larger).

Table ES-4 summarizes the performance of the hand-held system on shallow AP mines. The TNT thresholds used in the analysis were set on the day of the test; the RDX

thresholds were set after the test, based on a desired false-alarm rate. The *FAR* performance in this test could have been improved if more time had been spent on the lane survey.

Table ES-4. A Summary of the Hand-Held System's Shallow AP Performance

Shallow Antipersonnel Test Summary

Scan Type	<i>FAR</i> (m ⁻²)	<i>P_d</i>	Survey Speed
TNT (thresholds set at test)	0.22	1	16 min/m ²
RDX (new thresholds applied)	0.01	1	

DEEP ANTIPERSONNEL MINE DETECTION

The final test evaluated hand-held system performance against deep AP mines. Thirteen points were identified on the ground with a pair of markers separated by about 1 m. Seven of the points were located above PMA-1A mines, while the remaining points were devoid of mines. No RDX mines were tested. The distance between the top of the mine and ground surface was 2 cm. The markers were placed so that the mine was at a random position between the markers. A 2- by 8-cell grid was placed between the flags by the contractor, and each of these 16 cells was interrogated for mines (the cell size was again based on the detector's footprint). The contractor was allowed to re-interrogate any footprint. In some cases cells were interrogated three times, and in others a re-interrogation was made between the original cell positions to help in the detection process. The operators at the test determined when and where to make declarations.

Table ES-5 summarizes the performance of the hand-held system on deep AP mines. The TNT thresholds were set on the day of the test. If more time had been spent on the survey, the *FAR* and *P_d* results would have improved.

Table ES-5. A Summary of the Hand-held System's Deep AP Performance

Deep Antipersonnel Test Summary

Scan Type	<i>FAR</i> (m ⁻²)	<i>P_d</i>	Survey Speed
TNT (thresholds made at test)	4.3	0.86	19.2 min/m ²

CONCLUSIONS

- The tests summarized herein are the first wide-area tests of this early stage NQR detector. As such, the results obtained in the AT vehicular tests and the shallow AP handheld system tests were commendable, although the deep AP handheld test results need to be improved.

- Improvements in RFI mitigation, coil design, and search techniques should be pursued by the contractor to improve the sensitivity and speed of the detection process.
- Future systems will be much more than a repackaging of the current hardware. A vehicle system will have to maintain a reasonable rate of forward progress in order to be effective, and a hand-held unit must be reduced in size and weight so that it is man portable. These requirements may stress the system and degrade performance. On the other hand, advances in the fundamental detection approach may help to offset the above concerns.
- Future test procedures based on actual mine detection protocol will be more difficult than those used in these tests.
- This set of tests was limited in scope: (1) very few mine models were tested, and there were very few encounters of each mine model; (2) mines were buried in a limited range of depths; and (3) the lane areas were not large enough to accurately measure all the relevant quantities.
- The AP test results were separated into shallow and deep categories. In reality, this kind of separation is contrived because a demining effort in an area containing AP mines will likely encounter both deep and shallow mines. In a real scenario, low thresholds would likely have to be set to remain sensitive to deeper mines.
- Although reasonable projections were made to estimate the performance of future systems, only future testing of mature NQR systems will accurately determine their ultimate capabilities.

I. INTRODUCTION

A. TEST BACKGROUND

This report summarizes the results of an interim test of a system that uses the nuclear quadrupole resonance (NQR) signature of explosives for the detection of antipersonnel (AP) and antitank (AT) landmines. The system, designed and built by Quantum Magnetics, Inc., of San Diego, California, has been funded by the Defense Advanced Research Projects Agency (DARPA) Dog's Nose Program to develop technologies using chemical-specific approaches to the detection of explosives. The DARPA program is funding efforts to detect bulk as well as vapor-phase explosive; the NQR approach falls within the former category.

Currently, the armed Services use the AN/PSS-12 hand-held pulsed-induction metal detector for mine detection. The PSS-12, while effective against mines with high metal content, is less sensitive to plastic-cased mines, which contain only a modest amount of metal (usually located in the firing mechanism). Furthermore, any metal detector is, by nature, subject to false alarms from metallic clutter often present in areas where mine detection is a concern.

The tests discussed herein, performed the weeks of October 25 and November 29, 1999, took place at the DARPA Test Site at Fort Leonard Wood near St. Robert, Missouri. The Quantum Magnetics system was tested against AP and AT mine models buried in a set of test lanes. The AT mines were either plastic or metal cased and filled with either TNT or Comp B (which is a roughly equal mixture of TNT and RDX); the AP mines were plastic cased and filled with either TNT or RDX. Although the system tested here was a hand-held device, the goal of the test was to understand the current state of effectiveness that the NQR system would have as both a vehicle-mounted and hand-held system. Specifically, the test addressed three capabilities:

1. How a vehicle-mounted system would perform on AT targets
2. How a hand-held system would perform on shallow AP targets
3. How a hand-held system would perform on deep AP targets.

B. THE NQR APPROACH TO MINE DETECTION

The NQR approach to mine detection exploits the interaction of the quadrupole moment of ^{14}N (a prevalent element in explosives) with the electric field gradient of the crystal's electron cloud in the vicinity of the ^{14}N nucleus. The following discussion presents an intuitive classical explanation of this interaction; a rigorous quantum mechanical treatment can be found in the literature.¹

Nuclei with spin $I \geq 1$ have an asymmetrical charge distribution, thereby implying that the nucleus has an electric quadrupole moment. ^{14}N , whose spin is $I = 1$, falls into this category. The parameter Q is defined as a measure of the nuclear charge distribution's deviation from spherical symmetry. A nucleus with a nonzero Q possesses a quadrupole moment of eQ , where e is the unit electric charge. Values of $Q > 0$ imply that the major axis of the nucleus is aligned with the spin; for $Q < 0$ the minor axis of the nucleus is aligned with the spin. (It can be said that the former spins like a football, while the latter spins like a Frisbee). Figure I-1(a) shows a schematic of ^{14}N .

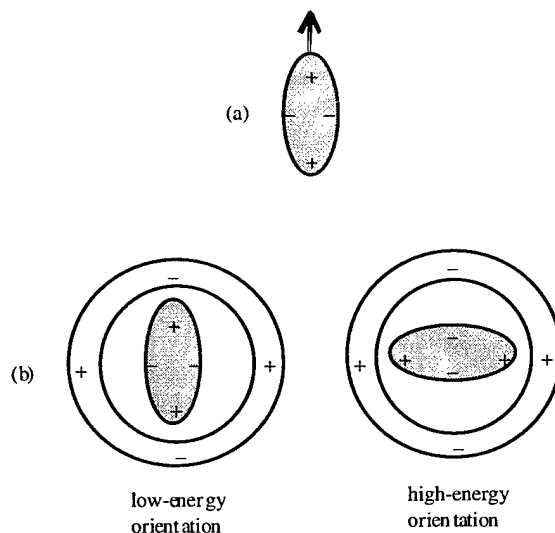


Figure I-1. (a) A Schematic View of a Quadrupole Nucleus. (b) The Low-Energy and High-Energy Configurations of a Quadrupole in an Electric Field Gradient.

The electrostatic energy of a charge distribution in an external electric potential can be written as an expansion that reveals how the multipoles interact with the external potential.² The terms in the expansion correspond to the total charge coupling to the

¹ H.G. Dehmelt, *Amer. J. Phys.* **22**, 110, 1954.

² See, for example, J.D. Jackson, *Classical Electrodynamics*, John Wiley & Sons, New York, 1975, p. 142.

potential, the dipole coupling to the electric field, the quadrupole coupling to the electric field gradient, and so on. Thus, a nucleus with a quadrupole moment will have an interaction energy with an electric field gradient, and if this nucleus is in a crystal, the interaction is the same for all the nuclei. Figure I-1(b) shows an example of a low-energy and high-energy orientation of a quadrupole in a hypothetical electric field gradient.

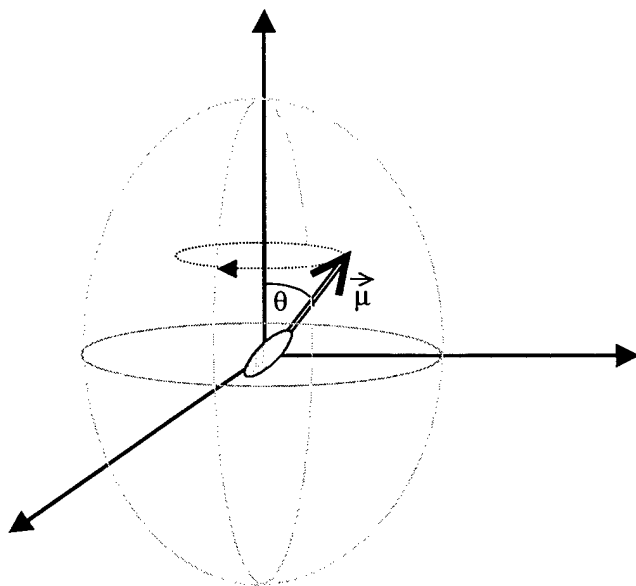


Figure I-2. The Interaction of a Nuclear Quadrupole with an Axially Symmetric Field Gradient

Consider the case of a quadrupole located in an axially symmetric electric field gradient that is described by ϕ_{zz} at the origin, as depicted in Figure I-2. It can be shown that the energy of this system is given by

$$E = \frac{eQ\phi_{zz}(3\cos^2\theta - 1)}{8}, \quad (\text{I-1})$$

where θ is the angle defined in the figure.³ Because of the dependence of the energy on θ , a torque results that tends to align the nuclear axis with the z (molecular) axis. The nucleus' angular momentum, which is aligned with the nuclear axis, will respond to the torque by precessing about the z axis.

Note that spin in Figure I-2 could equally well be oriented in the $+z$ or $-z$ direction in the ground state of the system, because both of the orientations have an equal energy [see Figure. I-1(b)]. This is, in fact, the case when the system is in the ground

³ H.G. Dehmelt, *ibid.*

state, and thus the ground-state system has no bulk magnetic moment (the moments sum to 0).

Now consider a magnetic field that is intended to bring the system into an excited state. A field $\mathbf{B} = \hat{x}B_0 \cos \omega_p t$, where ω_p is the NQR precession frequency, would exert a torque

$$\boldsymbol{\tau} = \boldsymbol{\mu} \times \mathbf{B} \quad (\text{I-2})$$

on the magnetic moments in the substance. Figure I-3(a) shows how the upward-oriented μ_+ (downward-oriented μ_-) are driven towards (away from) the positive y direction. If the magnetic field is terminated after the moments have "tipped" an angle of $\pi/2$, then the result is that shown in Figure I-3(b). In fact, it is the product $\mathbf{B}dt$, where dt is the time for which the field is applied, that determines the actual tip angle. Note that the moments in Figure I-3(b) will be then be rotating about the z axis in the x-y plane, creating an alternating magnetic field of their own in the x direction and at the original precession frequency. This is the NQR signal that is sought for mine detection.

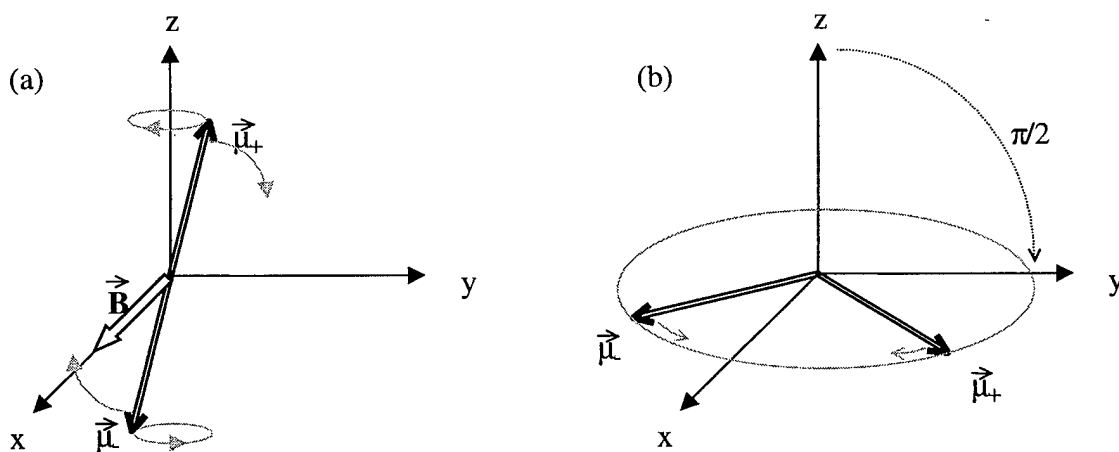


Figure I-3. (a) The Torque of an Alternating Magnetic Field at the NQR Frequency on the Magnetic Moments Precessing about the z-Axis in the Explosive Sample. (b) The Moments Rotating in the x-y Plane is the Result of a $\pi/2$ Rotation of the Moments.

We reiterate that the classical picture presented above is intended to provide insight into the physical effect of NQR spectroscopy, but should not be taken as a rigorous explanation.

It is natural to ask whether there are any clutter sources that could mimic the NQR signal of TNT or RDX. Examination of Eq. I-1 shows that the precession frequency (or the quadrupole resonance frequency) is critically dependent on ϕ_{zz} and Q , and thus the

frequency is essentially unique to that substance. Although it is theoretically possible for two substances to share the same resonance frequency (i.e., share the same product $\phi_z Q$), the probability is unlikely; over 50 years of research in NQR has not yielded a clutter source for either TNT or RDX that is known to the mine detection community.

This simplified picture of NQR presented above is complicated by the fact that explosives such as TNT and RDX are polycrystalline, that is, the explosives are aggregates of many randomly oriented crystal grains. This means that an applied field, such as that shown in Figure I-3, will not always be aligned along the same crystal axis throughout the explosive sample, and the effective torque applied to those nuclei is less than it would be in a single crystal, as shown in the figure. Consequently, it is necessary to produce a larger Bdt to obtain an effective tip angle of $\pi/2$ in a polycrystalline substance. A further consequence of the polycrystalline sample is the reduced signal that results from the differing orientations in the aggregate sample.

There are important time constants associated with the NQR process. The first time constant, T_1 , due to spin-lattice interactions in the system, defines the period over which the system returns to its thermal equilibrium state. The system must be re-excited to make more NQR measurements after T_1 has elapsed. There are mechanisms at work, however, that cause the NQR signal to degrade while the system is still excited (in other words, they degrade the signal before T_1 has elapsed). One mechanism, known as the spin-spin interaction, is the consequence of slight magnetic field differences seen by each nucleus that result from the spins in the lattice. This mechanism causes the rotating moments displayed in Figure I-3(b) to dephase to the point that there is no net magnetization left in the system. The time constant associated with this process, T_2 , is less than T_1 for the substances discussed herein. The other mechanism results from imperfections in the crystal that causes each nucleus to experience a slightly different electric field gradient. This means that the moments depicted in Figure I-3(b) will rotate at slightly different frequencies, again causing the moments to dephase. This time constant, T_2^* , is less than T_2 and thus dominates the signal's decay (called the *free-induction decay*). Table I-1 gives the parameters for TNT and RDX. These parameters are temperature dependent.

There is an important difference between the mechanisms that cause T_2 and T_2^* : the former is random effect, while the latter is a constant field-gradient perturbation at the sight of the nuclei. Because the cause of T_2^* is constant, it is recoverable in cases when there is a large difference between T_1 and T_2 (as in TNT). For example, if an additional

Table I-1. NQR Parameters for TNT and RDX.
These parameters depend on temperature.

	TNT	RDX
NQR Frequency	842 kHz	3.41 MHz
T_1	~5 sec	~15 msec
T_2	~100 msec	~5 msec
T_3	~2 msec	~0.5 msec

field is applied to the sample after the free-induction decay is complete, and the new field rotates the dephased moments of Figure I-3(b) by an angle of π , then the moments will begin to rotate in the opposite direction, and they will eventually become in phase with one another. The common analogy used to explain this is a group of unequal runners that begin a race together but slowly spread out (dephase) on the track. If the runners then, simultaneously, reverse directions, they would all reach the starting line at the same time. In the case of systems where T_1 is not that much greater than T_2 (as in RDX), other techniques are used to enhance the measurement.

C. HARDWARE CONFIGURATION USED AT THE TEST

The Quantum Magnetics system is currently configured to detect TNT and RDX, the two most common explosives used in landmines.⁴ The NQR frequencies used for these substances are about 842 kHz and 3.41 MHz, respectively. Because no other known substances have the same NQR resonance frequencies, there are no known clutter sources that could cause false alarms in the system. The system is limited, however, by radio frequency interference (RFI) sources that can reduce sensitivity and cause false alarms. This is especially true of TNT, whose resonance near 842 kHz is located in the AM radio band.

Although the majority of AT and AP mines worldwide have plastic cases, roughly 40 percent of all mine models manufactured to date have metal cases.⁵ Because the RF energy of the NQR system cannot penetrate a closed metal (conducting) container, the system was also designed to serve as a metal detector that operated with a high threshold to detect metal-cased mines without being too sensitive to small metallic clutter. In this

⁴ Quantum Magnetics is researching the feasibility to detect tetryl, a less common mine explosive.

⁵ Based on a search of the MineFacts CD database, compiled by the U.S. Department of Defense using data provided by the National Ground Intelligence Center, Charlottesville, Virginia. The actual fraction of metal-cased mines emplaced in a specific region will depend on the mine inventory available to the combatants who operated in that region.

way the system could potentially be used against the spectrum of plastic and metal-cased mines.

The system used at the tests consisted of a hand-held search head tethered to an electronics trailer that was towed by an automobile. The diameter of the search head's circular coil was 40 cm, although its effective footprint (or "sweet spot") was a circle of diameter 14 cm.⁶ The same search head was used to transmit (excite the NQR modes) and receive. Note that the footprint, which was determined by the magnetic field strength generated by the coil, was not a step function in radius, hence some nuclei outside the 7-cm radius were excited when the system radiated. The electronics trailer, which was powered by a portable diesel generator, contained the signal-processing and data-acquisition hardware. An RFI-mitigation system was also implemented during the test. It consisted of RFI-mitigation software and a multi-axis antenna to detect ambient RF energy. Figure I-4 shows the system.



Figure I-4. The Quantum Magnetics NQR Test at Fort Leonard Wood. The electronics trailer and vehicle are pictured on the right. The search head (marked by the white arrow) is resting on the ground beneath the white tent behind the trailer. The AT test lane is located on the left. The black plastic covering has been pulled off of the lane to reveal contractor declarations, marked by poker chips, so that they could be surveyed by test personnel. The RFI mitigation hardware and diesel generator are not shown in the picture.

⁶ The footprint size was established by requiring that the net sensitivity of a point located a footprint's radius off the center of the coil (which would be interrogated twice) would equal the sensitivity for a point at the center of the coil (which would only be interrogated once).

More detailed descriptions of the NQR method and hardware have been published by Quantum Magnetics.⁷

The system was brought to the vicinity of the test lanes by the vehicle, and the search head was carried and positioned by an operator to perform the lane survey. The search head tether was long enough so that it could be used to survey a reasonable area without having to move the electronics trailer and vehicle. The operator placed the search head on the ground at the desired position and interrogated that position with TNT, RDX, and metal scans. The TNT, RDX, and metal responses were measured at each position and recorded on a computer disk. If any response exceeded a predetermined threshold, either a mine declaration was made at that position, or the position was interrogated again. The actual method used was determined by the application, as will be discussed below when the specific tests are outlined. If the re-interrogation of a position was called for, the contractor ensured that a sufficient time delay elapsed before the re-interrogation was executed. This delay allowed the nuclei that were excited by the previous RF pulse to return to equilibrium so that they could be excited again. Although this delay (defined by the T_1 relaxation time) is only tens of msec for RDX, it can be almost 10 seconds for TNT. This did not affect the shallow AP test because of the survey method discussed below, but it was an issue in the deep AP test (and may be an issue in the future use of the system).

D. MEASURES OF EFFECTIVENESS

The detection probability (P_d), false-alarm rate (FAR), and rate of advance are the primary measures of effectiveness used in blind test analyses for mine detection. P_d is defined as the fraction of mines encountered that were detected. FAR is the number of false alarms per square meter. The rate of advance can be either be stated as the forward speed of the survey process (as typically applied to a vehicular system) or as the number of square meters surveyed per minute (as applied to hand-held systems).

The methods used to compute these measures in this report are test dependent and summarized in the chapters addressing the individual test results. The analysis goal was to understand both vehicle-mounted and hand-held system performance, but the

⁷ A.D. Hibbs, et al., "Detection of TNT and RDX Landmines by Stand-off Nuclear Quadrupole Resonance," *Proc. SPIE* **3710**, 454 (1999); "Man-Portable Mine Detector Using Nuclear Quadrupole Resonance: First Year Progress and Test Results," *IEEE Conf. Publ. No. 458*, 138 (1998); and "Landmine detection by Nuclear Quadrupole Resonance," *Proc. SPIE* **3392**, 522 (1998).

contractor used a hand-held system in all tests. Therefore, we used different approaches to the analysis.

II. ANTITANK MINE TEST RESULTS

A. TEST PROCEDURES

Is it feasible for NQR to detect AT mines in a vehicle-mounted configuration? The first test was designed to address this question. The test lane was sectioned into three arrays of cells: 8 by 72, 8 by 24, and 8 by 96. The cell length and width was set equal to the device's effective footprint diameter of 14 cm, hence the total lane dimensions were 1.12 m by 26.88 m, for a total area of about 30 m². The first two lane sections were called the east lanes, and the third section was called the west lane. The test contained 1 TMM-1, 2 Type 72, and 20 TMA-4 mines. Each mine was buried under dirt such that the top of the mine was between 2.5 and 5 cm below the ground surface. The mines were randomly distributed in the lane (they were not positioned relative to the established cell locations). Table II-1 contains details on these mines.

Table II-1. Summary of the AT Mines Used in the Test.
d is diameter, and h is height.

AT Model	Case Material	Main Charge	Size (cm)	Country of Origin
TMA-4	plastic	5.5 kg TNT	d = 28.4, h = 11	former Yugoslavia
Type 72	plastic	5.4 kg TNT/RDX (50.50)	d = 27, h = 10	China
TMM-1	metal	5.6 kg TNT	d = 30, h = 9	former Yugoslavia

Black opaque plastic was used to cover the lane so that the contractor could not see visual cues where the soil was disturbed during the mine burial process. To assist the contractor with search head placement, eight red strings, which defined the eight cross-track cells, were strung above the black plastic. Tape measures were also set down along the red string so that the along-track distance could be easily determined. The red string and tape measure enabled the contractor to quickly place the search head at the desired location in the lane. The search head was physically placed on the ground for each interrogation.

The lane was interrogated in 8 cell by 24 cell sections. All the locations along a 24-cell length, called a *grid*, were interrogated before moving on to the next grid. Cells

grid 8 →

grid 2 →

grid 1 →

1 7 13 19 2 8 14 20 3 9 15 21 4 10 16 22 5 11 17 23 6 12 18 24

24 cells

8 cells

Each cell in the grid was scanned for TNT, RDX, and metal, and these values were compared against preset thresholds. The time over which data was collected was 1 sec for RDX and about 0.25 sec for TNT. When the scan's measurement exceeded the threshold, a declaration or "hit" was attributed to that cell. Declarations were made based on a single interrogation, in the same way a future vehicle-mounted NQR system is expected to operate.⁸ Declarations were marked by cutting a small slit in the plastic at the center of the cell and inserting a poker chip onto the ground. The poker chips were surveyed after the test. In addition, the signal strengths of the TNT, RDX, and metal scans were recorded by a data-acquisition system and were made available for further analysis after the test was completed.

II-2

Note that this scanning procedure required the operator to disturb ground that had not yet been scanned (both by walking and resting the search head on it). Though clearly unsatisfactory for a hand-held detector scenario, this scanning procedure is not directly relevant to the NQR system in a vehicle-mounted configuration. The projected vehicle-mounted system would interrogate each piece of ground once and be configured such that the sensor precedes the vehicle on which it is mounted.⁹

The contractor used two different sets of thresholds for declaring mines on both RDX and TNT scans during this test. More conservative (lower) thresholds were used during the first day of testing, which covered the eastern portion of the lane; higher thresholds were used the second day in the west section. Because of this difference, we separate the analysis and results and compare the virtues of the lower and higher thresholds.

Two areas of the test lanes will not be included in the results: a 3 by 24 cell area at the end of the west lane was not completed because of lack of time, and a 2 by 24 cell area in the east section was excluded because of a technical problem encountered during the lane survey. The problem was realized when an unusually large fraction of cells (18 of the 48) recorded hits. The contractor determined and corrected the cause of the problem at the completion of this section.

B. ANALYSIS OVERVIEW

A vehicle-mounted NQR system is being considered as a route clearance system that would perform mine detection over long tracts of road. For the system to be effective in this role, a high P_d , low FAR , and reasonable rate of forward progress are all at a premium.

To estimate the performance of a hypothetical vehicular system, the results of the hand-held system test at Fort Leonard Wood must be appropriately projected. In this analysis, we consider the results of the hand-held system on a per-footprint basis and project them to a large, vehicular search head.

To move ahead with this projection, assumptions must be made about the vehicle system's hardware. Specifically, changing a small, hand-held search head to a large, vehicle-mounted head may change the signal-to-noise (S/N) characteristics of the coil.

⁹ Moreover, future vehicle-mounted systems are often discussed as having a mine overpass capability; whether this is reasonable is outside the scope of this document.

For example, a larger coil would see a larger signal from an AT mine for several reasons. First, the 14-cm diameter footprint coil used in the test excites only part of the explosive in an AT mine (whose diameter is typically 30 cm); a larger coil could excite the entire mine. Second, a larger coil is more likely to radiate an AT mine more uniformly in the vertical dimension, thereby maximizing the NQR signal from the mine. As an example, $|B|$ generated on the axis of a circular loop of current is proportional to $R^2/(R^2 + Z^2)^{3/2}$, where R is the loop's radius and Z is the on-axis (vertical) distance from the plane of the loop. It follows that $|dB/dZ| \propto 3R^2Z/(R^2 + Z^2)^{5/2}$, and the maximum fractional magnetic field inhomogeneity is reached at $Z = R$, as seen in Figure II-2. Given that a typical AT mine is 11 cm tall and is buried with about a 5-cm overburden, it follows that a large-radius coil would radiate AT mines more uniformly than a smaller coil because AT mines would be located at a distance Z that is a smaller fraction of the loop's radius. Third, a larger coil has more area in which to integrate magnetic field flux, making it more effective as a receive antenna. On the other hand, the disadvantage of a larger antenna is that it also has an increased response to RFI. Other design considerations will also influence the S/N comparison, including the power in the coil during radiation, the coil's shape (and thus the shape of its magnetic field), and ground effects.

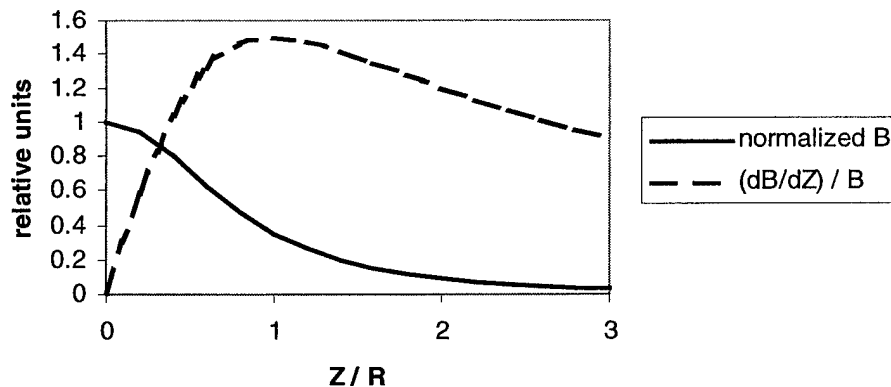


Figure II-2. The On-Axis Magnetic Field Strength (normalized) and Inhomogeneity ($dB/dZ/B$) for a Simple Wire Coil of Radius R . Note that the field is least homogeneous at $Z = R$.

The vehicle-mounted configuration is currently in the design phase. Quantum Magnetics, using models of NQR system hardware, intends to construct a vehicular system with an array of search coils, each of which is intended to have an S/N comparable to the coil used in this test. The coil size is to be determined. Given this, we will analyze the per-footprint results of this test and apply them to the hypothetical vehicle system.

Declarations in this test tended to “clump” in the vicinity of mines because more than 1 cell (footprint) overlapped with the AT mines (recall the footprint was 14 cm in diameter, while the typical AT mine is 30 cm in diameter). Declarations that were not near a mine tended to be isolated, because the false alarms were due to noise and RFI and were randomly distributed in position (they were not associated with a response to something in the ground). No clustering, however, was performed in the data analysis because a larger footprint vehicular search head would typically not “see” a mine multiple times as the smaller search head would, and so it is unlikely that clustering could be used effectively in a vehicular system.

C. FALSE-ALARM RATE PROJECTION

The *FAR* projected from this test is computed from the false-alarm probability (P_{fa}) for RDX, TNT, and metal scans as measured on a per-cell basis in the test. The relationship of these two quantities is given by:

$$FAR_{proj}^s = P_{fa}^s / A_{proj} \quad , \quad (II-1)$$

where A_{proj} is the area of the future vehicle’s cell and s denotes an RDX, TNT, or metal scan. The cell size is based on the footprint diameter, which has not yet been determined for the vehicle. Thus, A_{proj} is kept as a variable, not assigned a projected value. The false-alarm probability is given by:

$$P_{fa}^s = N_{fa}^s / N_{MT} \quad , \quad (II-2)$$

where N_{MT} is the number of cells that are “empty,” or devoid of the influence of a mine because they are not near a mine, and N_{fa}^s is the number of hits of scan s received within the N_{MT} empty cells. Because the cells are empty these hits are scored as false alarms.¹⁰

A distance criterion must be defined that separates cells that are near a mine from cells that are empty. Using the parlance of the field, we call this distance a “halo” of radius R_{halo} about the edge of the mine. Cells whose centers are outside the halo are considered “empty,” and hits in these cells are considered false alarms. We take R_{halo} to be 15 cm from the edge of the mine, consistent with the footprint of the detector.

¹⁰ Using these rules, the contractor would not be charged a false alarm for making a declaration of type $s = i$ near a mine of mine type $s = j$. This allows for the possibility that the detector could be sensitive to a small amount of metal in an otherwise low-metal mine or that there could be unknown RDX booster in a mine with a primary TNT charge. In any case, this conservative set of rules simply restricts the area from which the *FAR* will be measured, which will only modestly restrict statistics.

Table II-2 provides data, for both the east and west lanes, on the total number of cells interrogated, N_{MT} , N_{fa}^s , P_{fa}^s , and FAR_{proj}^s (which is the vehicle system's projected performance). Recall that FAR_{proj}^s is the only projected quantity—the other values were measured in the test. Note that the projected FAR for metal in the west lane is stated as an upper limit. We do this because there were no metal false alarms, so we can only conclude that, to a 90-percent confidence level (CL), there were fewer than 2.3 metal false alarms (it is not appropriate to conclude that the projected rate is 0).¹¹

Table II-2. Summary of the P_{fa} Measured in This Test as well as the Projected FAR for a Vehicular System Whose Cell Area, A_{proj} , Is yet to Be Determined. Results are listed for (a) the east lanes and (b) the west lane portion of the test. The declarations and thresholds used were chosen on the day of the test. See text for details.

(a) East Lanes

Scan	Total Cells in Lane	N_{MT}	N_{fa}^s	P_{fa}^s	FAR_{proj}^s
TNT	720	593	16	0.027	$0.027/A_{proj}$
RDX			3	0.005	$0.005/A_{proj}$
Metal			1	0.002	$0.002/A_{proj}$

(b) West Lane

Scan	Total Cells in Lane	N_{MT}	N_{fa}^s	P_{fa}^s	FAR_{proj}^s
TNT	696	526	8	0.015	$0.015/A_{proj}$
RDX			3	0.006	$0.006/A_{proj}$
Metal			0	0.000	$<0.004/A_{proj}$ (90% CL)

D. DETECTION PROBABILITY

A mine is normally considered to be detected if a contractor places a declaration within the distance R_{halo} of the edge of that mine. The results of scoring this test by the traditional definition should not be directly applied to a large-footprint vehicular system. In the test of the hand-held system, the small search head was placed directly atop a mine (such that its footprint was largely “filled” with explosive) more than once because its footprint is smaller than an AT mine's. Thus, the hand-held unit had more than one

¹¹ This upper limit on N_{fa}^{metal} is obtained from the Poisson probability distribution $P_n = \mu^n e^{-\mu}/n!$, where μ is the mean number of events and n is the observed number. Given that $n = 0$ for metal false alarms, the probability to find 0 events is $P_0 = e^{-\mu}$. A mean number $\mu = 2.3$ would give a 10-percent probability for P_0 . It is therefore said that $N_{fa}^{metal} < 2.3$ to a 90-percent confidence level.

opportunity to detect the same mine. This will likely no be the case for a vehicle coil footprint, which may be as large or larger than a mine.

Instead, we define P_d as the number of detections made in this test per opportunity. For the purposes of this report, an opportunity is defined as any footprint of the hand-held detector that intersected a mine such that the area of intersection was 90 percent of the detector footprint, as illustrated in Figure II-3. We call the number of such opportunities N_{full} , and the number of detections N_{det} . Hence, $P_d \equiv N_{det} / N_{full}$.

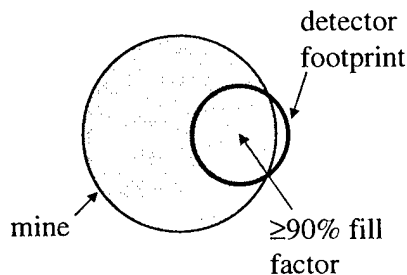


Figure II-3. Illustration of the 90-percent Fill-Factor Requirement to Determine per-Footprint Detection Probability

We chose a 90-percent fill factor because it represents a clear opportunity where a detection should have been made. In real-world detection scenarios there will be many cases where a mine is about split amongst two (or possibly up to four) footprints. Note, however, that although the detection probability for any one of those footprints will be low, there will be two (or up to four) opportunities for the mine to be detected.¹² Hence, for simplicity in the analysis, we take the P_d on 90-percent fill-factor footprints as representative of the overall performance.

Table II-3 lists N_{full} , the number of detections, and the measured P_d in the east and west lanes. We take this P_d as representative of the projected vehicle system as well, given the design goal for an S/N comparable to the system tested herein. Although the statistics on Type 72 and TMM-1 mines were low ($N_{full} = 1$), we will see in subsection F of this chapter that the RDX and metal scans have excellent sensitivity to Comp B and metal mines, respectively, and so a projected P_d of 1 is reasonable.

¹² As discussed earlier, this is how the contractor determined the 14-cm diameter footprint for the hand-held probe used in this test.

Table II-3. Summary of P_d Results on the East and West Lanes. The declarations and thresholds used were those determined on the day of the test. The scan type responsible for the detections are given in parentheses.

(A) EAST LANES

Mine Model	N_{full}	# detected (scan type)	P_d
TMA-4 (TNT)	13	13 (all TNT)	1.00
Type 72 (Comp B)	0	-	-
TMM-4 (metal)	0	-	-

(B) WEST LANE

Mine Model	N_{full}	# detected (scan type)	P_d
TMA-4 (TNT)	13	8 (all TNT)	0.62
Type 72 (Comp B)	1	1 (RDX&TNT)	1.00
TMM-4 (metal)	1	1 (metal)	1.00

E. ALTERNATE TNT THRESHOLD ON THE WEST LANE

TNT scans executed in the east lanes achieved a P_d of 1 (13/13) and a P_{fa} of 0.027; those in the west lane achieved a P_d of 0.62 (8/13) and a P_{fa} of 0.015. A potential explanation for this decrease in both P_d and P_{fa} is that a higher TNT threshold was applied to the data collected on the west lane. It is natural to ask whether applying the east lanes' threshold to the west lane's data would close the gap between the east and west results.

We applied the east thresholds to the west data offline and measured a P_{fa} of 0.053 and a P_d of 0.77. These results are not on par with the east lanes—the P_{fa} is larger and the P_d is lower. The decrease in performance might be due to a decrease in the S/N for the west lane, compared to the east. To check this, we made histograms of the TNT signal from the N_{full} cells and compared them to the signals from the N_{MT} cells, in both the east and west lanes (see Figure II-4). Note that the signal and noise distributions were more separated in the east lanes than in the west. It is not known what precisely caused the change in S/N performance.

F. RANGE OF SCANS

The distance over which TNT, RDX, and metal scans were sensitive was available in the data. Figure II-5 shows the response of these scans in all cells versus the miss distance between the cell center and mine center. Note that a miss distance of 21 cm

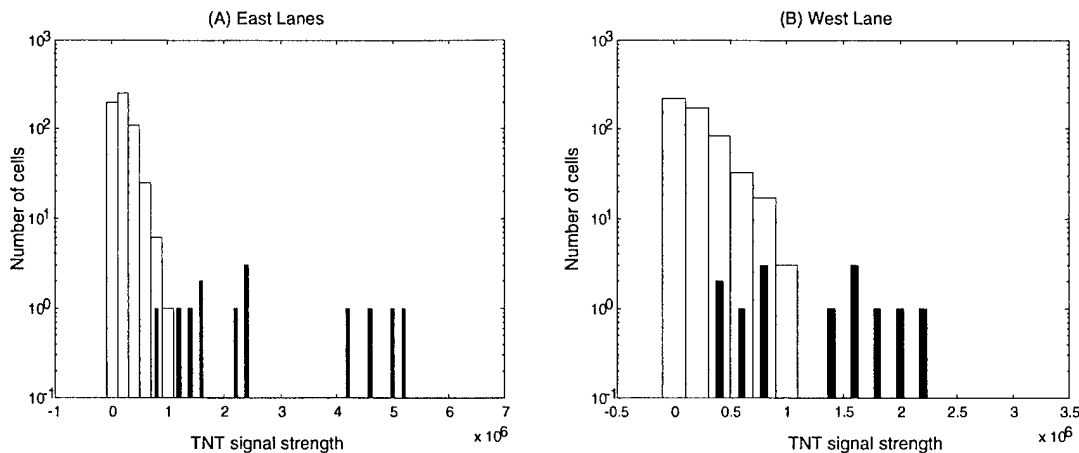


Figure II-4. TNT Signal Recorded for N_{full} Cells (black histogram) vs. N_{MT} Cells (white histogram). The signal and noise distributions (black and white, respectively) are better separated in the east than in the west.

corresponds to a situation where the edge of the mine and the edge of the detector's footprint touch, because a mine's radius is about 14 cm and the detector's footprint radius is 7 cm. Data for the TNT scans comes from the east lanes (this is where the TNT performance was best), while the RDX and metal plots were derived from the west lane. These plots show the detector's response to a mine (near a miss distance of 0 cm) compared to its noise (shown at miss distances > 30 cm), as well as at what miss distance a scan begins to pick up the mine signal. For TNT, a cell must be roughly within 10 cm of the center of a mine for its signal to be clear of the noise. For RDX and metal, the signal is in excess of the noise for cells as far as about 20 cm from the mine center. This strong RDX and metal performance gives confidence that P_d for these scans will be near 1 in a vehicle system, in spite of the poor statistics on N_{full} discussed earlier.

G. ISSUES AFFECTING VEHICLE SPEED

The vehicle speed will depend on the scan time, coil size, and number of coils mounted on the vehicle. Because the vehicle system has not yet been designed, it is impossible to predict the speed based on the results of this test. We can, however, point to some design issues that will influence the speed and effectiveness of the vehicle.

A vehicle system will have to cover roughly 3 m in the cross-track direction (perpendicular to the vehicle's forward motion); hence, it is likely that multiple coils will have to be used in the cross-track dimension. Multiple coils will likely be needed in the along-track dimension of the vehicle as well, because sensitivity to a given point on the ground must be maintained while the vehicle is in motion for the duration of the scan.

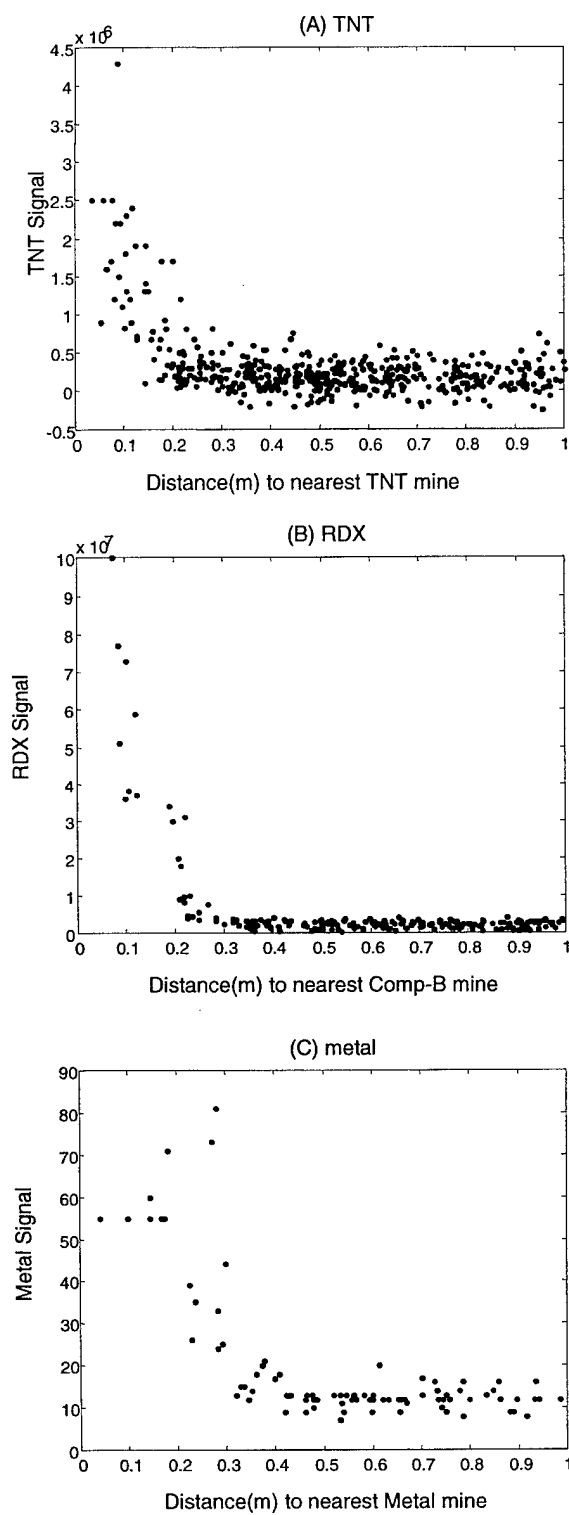


Figure II-5. (A) TNT, (B) RDX, and (C) Metal Signal Measured vs. Miss Distance to the Nearest Mine.

The system design must therefore account for potential pitfalls related to resonant coils operating in proximity to one another. It must further consider possible magnetic field leakage from the radiating coil into the ground outside of that coil; this leakage may cause signal degradation in the ground outside the coil. Last, if more than one coil is used to receive signals from a given point in the ground, there will be a noise contribution from both coils rather than just one. These issues may affect both TNT and RDX scans.

This list is not exhaustive; however, it brings to light some issues that must be addressed in the final vehicle design.

III. SHALLOW ANTIPERSONNEL MINE TEST RESULTS

A. TEST STRUCTURE

The second test measured hand-held system performance against shallow AP mines. The test lane was arranged to be 8 cells wide by 32 cells long. Again, the size of the cell edge was set equal to the effective footprint diameter (14 cm), so the total lane dimensions were 1.12 m by 4.48 m, or 5.02 m². The lane contained five VS-50 and seven PMA-1A mines; each mine in this lane was buried such that the top of the mine was roughly flush with the ground surface. Table III-1 contains details on these mines.

Table III-1. A Summary of the AP Mines Used in the Test. The quantities d, h, l, and w stand for diameter, height, length, and width.

AP Model	Case Material	Main Charge	Size (cm)	Country of Origin
PMA-1A	plastic	200 g TNT	l = 14, w = 7, h = 3	former Yugoslavia
VS-50	plastic	43 g RDX	d = 9, h = 4.5	Italy

This test's preparation and procedures were similar to the AT test procedures discussed above. An opaque black plastic sheet covered the lane so the contractor could not see where the soil was disturbed during the mine burial process. Eight red strings were strung above the black plastic to define the cross-track cell locations, and tape measures were set down along each grid so that the along-track distance could be easily determined during the test. A nonsequential interrogation scheme, similar to that portrayed in Figure II-1, was used by the contractor. The search head was placed on the ground at each survey location. Because this was a hand-held system test, multiple interrogations of a given footprint could be made. Initially, Quantum Magnetics planned to make a full survey of the lane, and then return to each hit cell to repeat the interrogation and confirm whether it should be a declaration. This is referred to as the *scan/confirm* scheme in this report. Only when both interrogations were hits would a declaration be made. Instead, the contractor recorded three complete independent surveys of the shallow AP lane. In this way a number of potential survey schemes could be investigated after the test.

A survey procedure that includes the additional interrogation of at least some footprints is needed when detecting AP mines, because the S/N on AP mines (especially TNT-filled) is small. It is necessary to set a threshold "into the noise" to effectively detect an AP-sized quantity of explosive. Rather than stopping at a single interrogation per cell and accepting the corresponding large *FAR*, a re-interrogation of those cells that exceeded threshold would reduce the effective *FAR* by an additional factor of P_{fa} (which is the false-alarm probability from a single interrogation).

As discussed above, this scanning procedure required the operator to walk and place the search head on ground that had not yet been scanned. Although unacceptable in a real mine-detection scenario, this procedure was allowed for this test because it was the first wide-area search performance for the contractor. It is important to note that the contractor is developing procedures where the operator will follow "behind" the search head, as well as keep the search head off the ground.

B. ANALYSIS OVERVIEW

Hand-held mine-detection systems are currently used for the detection of AP and AT mines, but vehicle systems will, when they are introduced, likely be expected to detect AT mines only. Consequently, we consider only a hand-held version of an NQR device for application to AP mines. Ultimately, a hand-held NQR system will be confined in weight and volume so that the electronics associated with the search head is backpack-portable—clearly a more advanced implementation of the hand-held unit tested here. Regardless, we will apply the results of the unit tested here as representative of the current status of AP mine detection using NQR.

In this report we will consider the results from the scan/confirm scheme; Quantum Magnetics can provide details on other survey approaches under consideration.¹³ Note that the scan/confirm approach is logically equivalent to computing the AND of pairs of complete single passes. Therefore, we show results of the scan/confirm approach based on the logical AND of the three single passes (1 + 2, 1 + 3, and 2 + 3). We use the TNT, RDX, and metal thresholds that were chosen on the day of the test.

¹³ We have chosen the scan/confirm scheme because it is fast: it requires the interrogation of all footprints once, and then an additional interrogation of only those footprints that exceeded a pre-set threshold. Other approaches that would require averaging two or three interrogations of every footprint, while potentially more effective, would slow the survey process considerably.

We apply simple clustering to the data before measuring detections and false alarms. Specifically, any hits whose cells were joined on an edge were grouped into one declaration whose position was defined as the geometrical center of the cluster of cells (the hits were not weighted by their signal strength in this implementation, even though this would seem like a worthwhile refinement). Hits joined by their corners were considered separate entities. The clustering that was performed, however, did not seem to materially affect the results below.

In this analysis we consider RDX and TNT to be orthogonal. Thus, an RDX declaration is considered a false alarm if it overlaps with a TNT mine and not with an RDX mine. We do not consider the metal signals because there were no metal measurements that exceeded preset threshold at the test. Note, however, that the metal signal did increase in the vicinity of the VS-50s and thus could have been exploited with a lower threshold.¹⁴ We used a miss distance of 20 cm as the critical distance that differentiated detections from false alarms. This distance is based on the 15 cm R_{halo} discussed above, and an average mine radius of 5 cm that is taken as the representative center-to-edge size of an AP mine. Thus, the area from which false alarms may be drawn is given by:

$$A_{fa}^s = A_{\text{lane}} - N_{\text{mine}}^s A_{\text{mine+halo}} \quad , \quad (\text{III-1})$$

where s is the scan type (RDX or TNT), A_{lane} is the total lane area (5.02 m²), N_{mine}^s is the number of mines (five RDX and seven TNT), and $A_{\text{mine+halo}}$ is the area of the mine plus halo ($\pi 0.2^2$). This leaves $A_{fa}^{\text{TNT}} = 4.14 \text{ m}^2$ and $A_{fa}^{\text{RDX}} = 4.39 \text{ m}^2$.

C. TNT FAR AND P_d

Figure III-1(a) shows the results of the three single passes of TNT scans on each footprint in the shallow AP lane. All hits, shown as gray and black squares, were grouped into clusters as discussed above. Black clusters were false alarms (the cluster center was not within R_{halo} of any TNT mine); gray clusters were detections. The TNT mines are shown as black dots superimposed on the plot.

Although all the TNT mines were detected in each of the single passes, the number of false alarms in the single pass approach is large. In fact, the number of false-

¹⁴ The VS-50 is a plastic-cased mine, but it is available, as specified by the customer, with either a plastic or metal reinforcing plate in its pressure pad. It is the authors' experience that most VS-50s used for testing in the United States contain the metal plate, judging from the large metal signal generally measured over the mine. Details on the VS-50 can be found in *Jane's Mines and Mine Clearance* (Surrey, UK: Jane's Information Group Limited, 1998) p. 169.

alarm clusters in pass 1, pass 2, and pass 3 was measured to be 17, 7, and 14, respectively. Figure III-1(b) shows the results of the scan/confirm approach. Clustering was done after the AND was performed on the single passes. Clearly, the confirmation step was crucial: all the TNT mines were still detected in each case, but the number of false-alarm clusters was reduced to 0, 0, and 2 in the three combinations constructed. Table III-2 gives the FAR and P_d results of these runs.

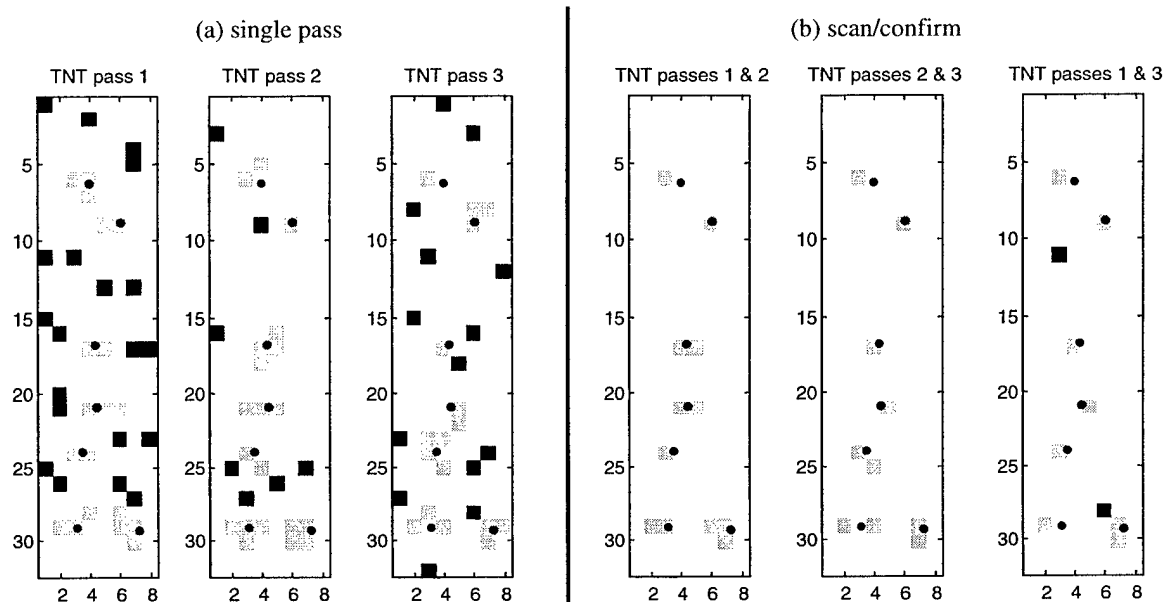


Figure III-1. Results of Single Passes (a) and Scan/Confirm Scheme (b) on Seven PMA-1A TNT-Filled AP Mines. Grey clusters are detections and black clusters are false alarms. Black dots mark the locations of the mines. The TNT threshold used was chosen on the day of the test.

Table III-2. Summary of the TNT Results. The TNT threshold used was chosen on the day of the test.

	Measured $FAR (m^{-2})$	Measured P_d
TNT 1 and 2	0	1
TNT 1 and 3	0	1
TNT 2 and 3	0.48	1

Ideally, the AP lane would have been large enough to allow for accurate measurements of the scan/confirm FAR for TNT. For example, a single false alarm translates to a FAR of $1/A_{fa}^{TNT} = 0.24 m^{-2}$. It is clear from Table III-2 that this is about the rate we are trying to measure. It may instead be better to estimate the FAR for the scan/confirm method from the single-pass results. Using a similar approach to that developed for the AT test (cf. with Eq. II-1 and II-2), we have:

$$FAR_{\text{estimated}}^s = (P_{fa}^s)^2 / A_{\text{cell}} \quad , \quad (\text{III-2})$$

where P_{fa}^s is the false-alarm probability for a single pass, given by:

$$P_{fa}^s = N_{fa}^s / N_{MT}^s \quad . \quad (\text{III-3})$$

N_{MT}^s is again the number of empty cells, but is now dependent on the scan s in the AP analysis. We use a miss-distance of 20 cm between the center of an AP mine and the center of a cell to determine which cells are in the “empty” category. $N_{MT}^{\text{TNT}} = 209$ and, taking an average of the three single passes, $N_{fa}^{\text{TNT}} = 13.67$ (20 from pass 1, 7 from pass 2, and 14 from pass 3, ignoring clustering), giving $P_{fa}^{\text{TNT}} = 0.065$. Thus, the estimated FAR for TNT scans is $FAR_{\text{estimated}}^{\text{TNT}} = 0.22 \text{ m}^{-2}$. Note that this is consistent with the results in Table III-2, and is probably the best representation of the average rate.

D. RDX FAR AND P_d

Figure III-2 shows the results of the three single passes of RDX scans on each footprint in the shallow AP lane. All the symbols on this figure are the same as those in Figure III-1. In addition, however, one mine in each of passes 2 and 3 are shown circled, because these were not detected using the threshold set at the test. The scan/confirm approach is not shown for this RDX data because mines were missed in these lanes using this threshold.

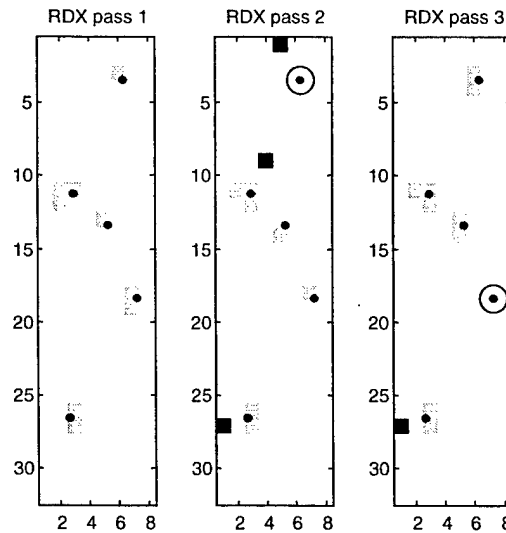


Figure III-2. Results of Single Passes on Five VS-50 RDX-Filled AP Mines. Grey square clusters are detections; black square clusters are false alarms. Black dots are the 5 mines, and circled dots are mines that were not detected. The RDX threshold used here was chosen on the day of the test.

Although the RDX FAR was admirably low in the single passes shown in Figure III-2, the RDX threshold was probably too high, given the missed mines in passes

2 and 3. In spite of the potential of this system for single-pass detection of RDX, we consider it in a scan/confirm mode and aim for RDX results that are good enough so that TNT scans will dominate the *FAR* (as well as the time spent in the process of re-interrogating footprints). For example, we consider the goal of an RDX *FAR* of 0.01 m^{-2} . This *FAR* is essentially negligible compared to the estimated TNT *FAR* of 0.22 m^{-2} discussed above. According to Eq. III-2, P_{fa}^{RDX} should be set to 1.4 percent for this goal to be met in the scan/confirm scheme. Figure III-3 shows a histogram of RDX data from pass 1 for all $N_{fa}^{\text{RDX}} = 225$ cells not within the R_{halo} of a VS-50. A P_{fa}^{RDX} of 1.4 percent would correspond to about a 1,380,000 threshold in RDX signal strength, which is 20 percent lower than the RDX threshold set at the test. Figure III-4 shows the effect of this new threshold on the RDX data. All the RDX mines were still detected in each scan/confirm case shown in (b) on the figure, while the number of false-alarm clusters was reduced to 0, 0, and 1 in the three scan/confirm combinations constructed from the individual passes. Table III-3 gives the *FAR* and P_d results of these runs. Note that given the estimated *FAR* of 0.01 m^{-2} , there should have been on average of 0.044 false alarms per scan/confirm case in Figure III-4(b), or, in other words, there should have been a total of 0.13 false alarm clusters in the sum of the three combinations. That the measured *FAR* is about 7.5 times this number is most probably just a statistical fluctuation with about a $0.13e^{-0.13}$, or 10-percent probability. As was the case for TNT, the lane is too small for the scan/confirm false alarm measurements, and the estimated RDX *FAR* of 0.01 m^{-2} is the best measure of the system performance in this lane.

E. SURVEY SPEED

Quantum Magnetics needed about 75 minutes to complete a single pass of the 5.02 m^2 shallow AP lane. In a realistic mine-detection scenario, the overall mine density will be quite low. Hence, the dominant reason for a confirmation scan will be to clarify a false alarm, and of those, most will be to clarify the TNT response. We can obtain a complete survey estimate by increasing the single pass time (75 minutes) by the fraction of cells that need TNT confirmation (given by P_{fa}^{TNT}), which was found to be 6.5 percent. We conclude that the total time to complete the shallow AP lanes using the scan/confirm method would be about 80 minutes, or about 16 minutes per square meter.

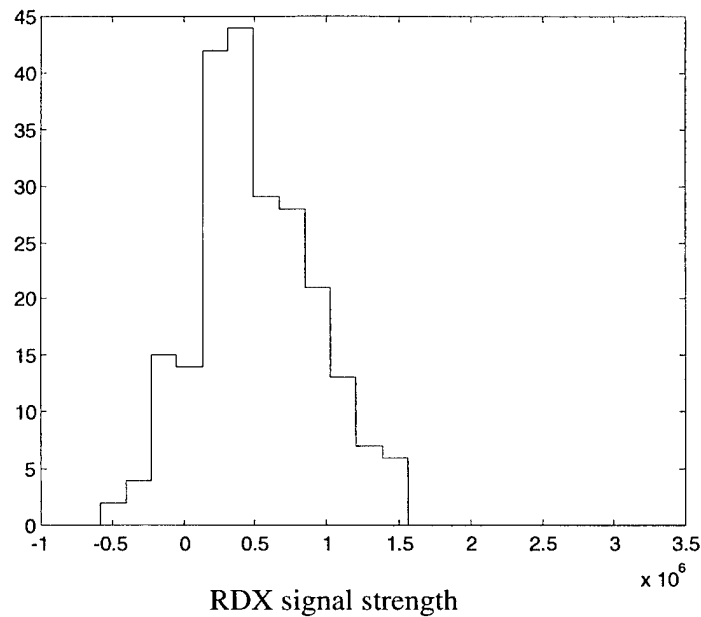


Figure III-3. Histogram of RDX Data for Footprints Not Near a VS-50. An RDX threshold of 1,380,000 would correspond to about a $P_{fa} = 1.4$ percent.

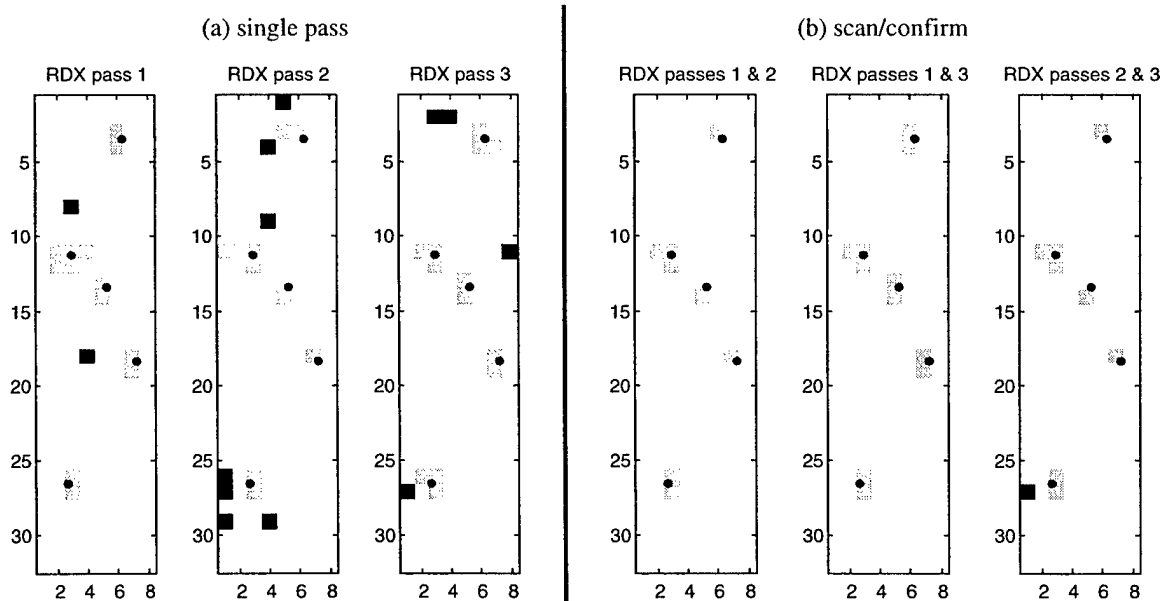


Figure III-4. Results of Single Passes (a) and Scan/Confirm Scheme (b) on Five VS-50 RDX-filled AP mines. Grey square clusters are detections; black square clusters are false alarms. Black dots are the mines. The RDX threshold was determined based on Figure III-3, as discussed in the text.

Table III-3. Summary of the RDX Results. The RDX threshold was based on a desired *FAR*, and chosen for the purposes of this report. See text for details.

	Measured <i>FAR</i> (m ⁻²)	Measured <i>P_d</i>
RDX 1 and 2	0	1
RDX 1 and 3	0	1
RDX 2 and 3	0.23	1

Note that this estimate is based on a test of very specific situation (shallow AP mines) and of a system that has not yet matured. There are compelling reasons that this time might increase or decrease. For example, improvements in the technology and survey technique could certainly lower this time estimate. On the other hand, real-world conditions (where mines are not so benignly shallow) will force the user to set a conservative threshold, thereby increasing the time spent in the confirmation process.

IV. DEEP ANTIPERSONNEL MINE TEST RESULTS

A. TEST PROCEDURE

The last test was concerned with hand-held system performance against deep AP mines. A pair of markers separated by about 1 m identified each of 13 points on the ground. Seven of the points were above PMA-1A mines, and the remainder were devoid of mines. The distance between the top of the mine and ground surface was 2 cm. The markers were placed so that the mine was at a random position between the markers. A 2-by 8-cell grid, made of a plastic frame and string, was placed between the markers by the contractor, and each of these 16 cells was interrogated for mines. As above, the cells were 14 cm squares, so a 28- by 112-cm area was searched at each position. The contractor was allowed to re-interrogate any cell. In some cases, cells were interrogated three times; in others, the detector's footprint was placed between cells to help in the detection process. The operators at the test determined when and where to make declarations, which were marked on the ground with a poker chip.

B. FAR

There were a total of eight declarations within the six locations that did not contain a mine. The total area encompassed by these six locations was 1.88 m^2 , hence the measured FAR was 4.3 m^{-2} .

C. DETECTION PROBABILITY

Of the seven mines encountered in this test, six were detected by declarations whose miss distance was within 20 cm of the mine's center (note that no declarations were placed on the grid above the missed mine). Thus, the measured P_d for this test was 86 percent. Note that there was a contribution to the P_d from accidental overlaps of false alarms, as estimated by $FAR \times A_{\text{mine+halo}}$, where $A_{\text{mine+halo}}$ is the area of the mine and halo (the area in which a declaration will be called a detection). Hence these accidental detections contribute to a P_d of $4.3 \times \pi 0.2^2$, or 0.54, on their own.

D. SURVEY SPEED

We can obtain a complete survey estimate by increasing the single pass time of the shallow AP test (75 minutes per 5.02 m²) by the fraction of cells that were re-interrogated for TNT confirmation (28 percent). We conclude that the total time to complete AP lanes that include deep mines is 19.2 minutes per m². Note that no additional time was added for TNT relaxation, so this estimate is probably a lower limit.

V. RESULTS SUMMARY AND CONCLUSIONS

A. VEHICULAR AT PERFORMANCE PROJECTIONS

Table V-1 summarizes the antitank performance estimates using a single 0.25-s TNT scan and a 1-s RDX scan. We have taken the east and west lanes results together in this summary (recall that the results of the two lanes were kept separate in Chapter II). Two estimates are presented for TNT: the first uses the TNT thresholds that were set each day at the test, and the second applies the more conservative, lower threshold (set at the test on the east lane) to both the east and west lanes. The variable A_{proj} is the area of the future vehicle system cell, which is based on the coil size (the coil is currently being designed).

Table V-1. A Summary of the AT Performance Estimates for a Vehicular System

Antitank Test Summary

Scan Type	$FAR (m^{-2})$	P_d
TNT (thresholds set at test)	$0.021/A_{proj}$	0.81
TNT (east threshold applied)	$0.039/A_{proj}$	0.89
RDX (thresholds set at test)	$0.0054/A_{proj}$	1
Metal (thresholds set at test)	$0.0009/A_{proj}$	1

B. HAND-HELD PERFORMANCE ON SHALLOW AP MINES

Table V-2 summarizes the performance of the hand-held system on shallow AP mines. The TNT thresholds were set on the day of the test; the RDX thresholds were set after the test, based on a desired FAR .

Table V-2. A Summary of the Hand-Held System's Shallow AP Performance

Shallow Antipersonnel Test Summary

Scan Type	$FAR (m^{-2})$	P_d	Survey Speed
TNT (thresholds set at test)	0.22	1	16 min/m ²
RDX (new thresholds applied)	0.01	1	

C. HAND-HELD PERFORMANCE ON DEEP AP MINES

Table V-3 summarizes the performance of the hand-held system on deep AP mines. Only TNT mines were tested; the TNT thresholds were set on the day of the test. If more time had been spent on the survey, the FAR and P_d results would have improved.

Table V-3. A Summary of the Hand-held System's Deep AP Performance

Deep Antipersonnel Test Summary

Scan Type	FAR (m^{-2})	P_d	Survey Speed
TNT (thresholds made at test)	4.3	0.86	19.2 min/ m^2

D. CONCLUSIONS

- The tests summarized herein are the first wide-area tests of this early stage NQR detector. As such, the results obtained in the AT vehicular tests and the shallow AP handheld system tests were commendable, although the deep AP handheld test results need to be improved.
- Improvements in RFI mitigation, coil design, and search techniques should be pursued by the contractor to improve the sensitivity and speed of the detection process.
- Future systems will be much more than a repackaging of the current hardware. A vehicle system will have to maintain a reasonable rate of forward progress in order to be effective, and a hand-held unit must be reduced in size and weight so that it is man portable. These requirements may stress the system and degrade performance. On the other hand, advances in the fundamental detection approach may help to offset the above concerns.
- Future test procedures based on actual mine detection protocol will be more difficult than those used in these tests.
- This set of tests was limited in scope: (1) very few mine models were tested, and there were very few encounters of each mine model; (2) mines were buried in a limited range of depths; and (3) the lane areas were not large enough to accurately measure all the relevant quantities.
- The AP test results were separated into shallow and deep categories. In reality, this kind of separation is contrived because a demining effort in an area containing AP mines will likely encounter both deep and shallow mines. In a real scenario, low thresholds would likely have to be set to remain sensitive to deeper mines.
- Although reasonable projections were made to estimate the performance of future systems, only future testing of mature NQR systems will accurately determine their ultimate capabilities.

REPORT DOCUMENTATION PAGE

Form Approved
OMB No. 0704-0188

Public Reporting burden for this collection of information is estimated to average 1 hour per response, including the time for reviewing instructions, searching existing data sources, gathering and maintaining the data needed, and completing and reviewing the collection of information. Send comments regarding this burden estimate or any other aspect of this collection of information, including suggestions for reducing this burden, to Washington Headquarters Services, Directorate for Information Operations and Reports, 1215 Jefferson Davis Highway, Suite 1204, Arlington, VA 22202-4302, and to the Office of Management and Budget, Paperwork Reduction Project (0704-0188), Washington, DC 20503.

1. AGENCY USE ONLY (Leave blank)		2. REPORT DATE March 2000	3. REPORT TYPE AND DATES COVERED Final — October 1999 – February 2000	
4. TITLE AND SUBTITLE Antitank and Antipersonnel Mine Detection Test Results for a Nuclear Quadrupole Resonance Detection System			5. FUNDING NUMBERS DASW01 98 C 0067 DARPA Assignment DA-2-1698	
6. AUTHOR(S) Frank S. Rotondo, Elizabeth Ayers				
7. PERFORMING ORGANIZATION NAME(S) AND ADDRESS(ES) Institute for Defense Analyses 1801 N. Beauregard St. Alexandria, VA 22311-1772			8. PERFORMING ORGANIZATION REPORT NUMBER IDA Document D-2444	
9. SPONSORING/MONITORING AGENCY NAME(S) AND ADDRESS(ES) DARPA 3701 North Fairfax Drive Arlington, VA 22203			10. SPONSORING/MONITORING AGENCY REPORT NUMBER	
11. SUPPLEMENTARY NOTES				
12a. DISTRIBUTION/AVAILABILITY STATEMENT Approved for Public Release; unlimited distribution (May 23, 2000).			12b. DISTRIBUTION CODE	
13. ABSTRACT (Maximum 180 words) This report summarizes the results of an interim test of a system that uses the nuclear quadrupole resonance (NQR) signature of explosives for the detection of antipersonnel (AP) and antitank (AT) landmines. The system, designed and built by Quantum Magnetics, Inc. of San Diego, California, has been funded by the Defense Advanced Research Projects Agency (DARPA) Dog's Nose Program to develop technologies using chemical-specific approaches to the detection of explosives. The tests discussed herein were performed the weeks of October 25 and November 29, 1999, at Ft. Leonard Wood, near St. Robert, Missouri. The Quantum Magnetics system was tested against AP and AT mine models buried in a set of test lanes. The AT mines were either plastic or metal cased and filled with either TNT or Comp B; the AP mines were plastic cased and filled with either TNT or RDX. This report outlines the current capability that is expected from both a vehicle-mounted and hand-held version of the NQR system.				
14. SUBJECT TERMS mine detection, explosives detection, nuclear quadrupole resonance			15. NUMBER OF PAGES 46	
			16. PRICE CODE	
17. SECURITY CLASSIFICATION OF REPORT UNCLASSIFIED	18. SECURITY CLASSIFICATION OF THIS PAGE UNCLASSIFIED	19. SECURITY CLASSIFICATION OF ABSTRACT UNCLASSIFIED	20. LIMITATION OF ABSTRACT SAR	